southern oval, active along its entire length, is pictured. The aurora occurs at a geomagnetic colatitude of about 23° at the top of the photograph, where the local time is midnight, and at about 14° geomagnetic colatitude at the bottom of the photograph, near local noon. In such photographs it is quite common to see, as in Fig. 1, a dimmer, diffuse auroral form on the side away from the geomagnetic pole and brighter, more sharply defined features on the side toward the geomagnetic pole. The minimum detectable signal in these photographs is about 8.5×10^{-10} watt cm^{-2} $ster^{-1}$. The system saturates at 8.5×10^{-9} watt cm^{-2} $ster^{-1}$. These spectral integrated fluxes correspond to about 43 and 430 kilorayleighs, respectively, along the center of the strip. The slant path at the edges of the photograph in Fig. 1 causes weak layers to appear brighter there than at the center of the strip. An instrumental problem caused the base line to be shifted by an unknown amount in the lower part of Fig. 1, when the spacecraft was illuminated by sunlight, thus suppressing the dimmer auroral features.

The aurora frequently displays an eddy-like form with a characteristic length of a few hundred kilometers, which can be seen to some extent in Fig. 1. Hasegawa (*5*) has suggested that this may be the result of kink instability in the field-aligned sheet current proposed by Akasofu and Meng (*6*).

Seven consecutive photographs, each taken near local midnight, were overlaid to form the composite shown in Fig. 2. The interval between adjacent photographs is 102 minutes, which is the orbital period of the satellite. The continuity, or lack thereof, at the boundaries indicates the variability of auroral activity in 102 minutes. The general location and intensity are fairly constant from frame to frame, but one sees dramatic changes in the fine structure. The most widely used index of geomagnetic activity, K_p, had a value of 3+ during the two photographs on the right, taken over the Atlantic Ocean and the East Coast of the United States, decreased to 3 during the time when the two photographs over central United States and the West Coast of the United States were taken, decreased to 2+ during the next two photographs, over Alaska, and to 1 at the time of the photograph on the extreme left. The correlation of auroral activity, as recorded by these photographs, with K_p is thus crude. The photograph on the extreme left shows the least geomagnetic activity and occurs at the time of lowest K_p, but the photographs over Alaska and the western United States appear to have no less geomagnetic activity, perhaps even more, than those over the eastern United States and the Atlantic, which were taken when K_p was greater.

Even when the clouds are illuminated by moonlight, one can usually distinguished the aurora from clouds by its location and shape, as shown in the cover photograph. The moon was one day past first quarter and was almost directly overhead, at the equator, when the cover photograph was taken. One can also distinguish the aurora from clouds by comparing a photograph taken with visible light with a simultaneous thermal infrared image, in which clouds are generally visible but the aurora is transparent, as shown in the cover photograph. This comparison is useful even when the moon is located so that no moonlight is reflected from the clouds, because it sometimes happens that the reflection of bright aurora from clouds can be confused with dim aurora. Note the fjords of northeastern Greenland as seen by reflected auroral light in the cover photograph.

Photographs taken from satellites make it possible to monitor auroral activity on a global basis. In addition to yielding valuable insight into the nature of the aurora, this coverage will permit more meaningful correlation of ground-based and satellite-borne experiments designed to unravel this complex phenomenon.

ERNEST H. ROGERS
DAVID F. NELSON
Space Physics Laboratory, Aerospace Corporation, Los Angeles, California 90009
RICHARD C. SAVAGE*
U.S. Air Force Weather Service, Scott Air Force Base, Illinois 62225

References

1. J. W. Chamberlain, *Physics of the Aurora and Airglow* (Academic Press, New York, 1961), pp. 151–216.
2. C. D. Anger, *Eos Trans. Am. Geophys. Union* **53**, 108 (1972).
3. Y. I. Feldstein and G. V. Starkov, *Planet. Space Sci.* **15**, 209 (1967).
4. A. Omholt, *The Optical Aurora* (Springer-Verlag, New York, 1971), pp. 7–18.
5. A. Hasegawa, *Phys. Rev. Lett.* **24**, 1162 (1970).
6. S. I. Akasofu and C. I. Meng, *J. Geophys. Res.* **74**, 293 (1969).

* Present address: Department of Meteorology, University of Wisconsin, Madison 53706.

21 May 1973; revised 23 July 1973

Low-Loss Niobium-Tin Compound for Superconducting Alternating-Current Power Transmission Applications

Abstract. *A Nb_3Sn superconductor has been fabricated in rods and tapes by the interaction of the tin contained in a copper-tin alloy with niobium which had been in contact with the alloy material. This conductor has lower alternating-current (60 hertz) losses than any presently available commercial products.*

The a-c loss of a type II superconductor at 60 hertz is one of the most important properties which determines the feasibility of using this material in superconducting a-c power transmission lines. The superconductor Nb_3Sn is of interest for this application primarily because it has a high superconducting transition temperature ($T_c \cong$ 18 K), a high critical field, and a high critical current density (*1*). Although the high critical current is important for overload conditions, for normal operation currents corresponding to peak surface fields of the order of 1000 oersteds are desirable. Under this operating condition, acceptable losses would be several $\mu w/cm^2$ (*1*).

The a-c losses and especially the effect of various metallurgical treatments on these losses (*2, 3*) have not, to our knowledge, been studied under conditions appropriate for this application. Out of the investigation reported here of the losses in Nb_3Sn has been developed a processing method for preparing Nb_3Sn conductors with losses that are substantially lower than previously available and that are more than adequate for the realistic designs discussed in (*1*). We report here a summary of this work.

To produce the required test specimens of Nb_3Sn, two fabrication methods were used: (i) "composite" and (ii) "tin dipping" processing. The first process is based on the method now used for making multifilamentary A-15 compound conductors (*4*). In this process a 0.64-cm niobium rod is inserted into a 1.27-cm copper-tin alloy tube approximately 15.3 cm in length, and this composite is then drawn to a 0.64-cm diameter. It is then sectioned into pieces 7.6 cm long for heat treatments. Encapsulated sections of the composite are heated for up to 400 hours at 700°C and 800°C. During these heat treatments, a single-phase Nb_3Sn layer is formed on the outer surface of the niobium rod as a result of the preferential reaction of tin with niobium. The thickness of the layer is normally 1 to 10 μm but in some cases it is as thick as 100 μm. When measuring the a-c losses, the copper-tin alloy matrix around the Nb_3Sn is chemically removed.

In the tin dipping process, one of the conventional methods of producing commercial Nb_3Sn conductors, a niobium rod (10.2 cm long and 0.32 cm in diameter) is dipped into a molten tin bath held in a vacuum at temperatures between 600° and 1000°C. A single-phase Nb_3Sn layer is formed on the outer surface of the niobium rod if the bath temperature is above 930°C. When the temperature is below 930°C, the dipped specimens require a subsequent heat treatment, which consists of encapsulation in quartz tubing and heating for 3 to 300 minutes at temperatures between 950° and 1000°C to form the single-phase Nb_3Sn layer on the niobium surface. The thickness of the layers was generally between 1 and 10 μm.

The a-c losses were measured electronically (*5*) by a method which is in principle very similar to one used by Easson and Hlawiczka (*6*). In this method a test sample (5.1 cm long) wound with 800 turns (two layers) of No. 46 Formvar copper wire is inserted in a small a-c superconducting solenoid. The solenoid produces a field parallel to the axis of the specimen which is uniform to better than 1 percent over the entire length of the sample. The experimental quantities $d\phi/dt$ and H are measured (ϕ is the total flux penetrating the superconductor and H is the applied field). The power loss, $\bar{P}$, per unit surface area is obtained by electronically averaging the product of $d\phi/dt$ and H since the loss can be expressed as

$$\bar{P} = \frac{1}{4\pi S\tau}\int_0^\tau H(d\phi/dt)\,dt$$

where τ is the period of H and S is the circumference of the specimen.

Measurements on representative samples prepared by both methods are summarized in Fig. 1. The losses are plotted as a function of the peak a-c magnetic field (in oersteds) and the induced root-mean-square surface current density (in amperes per centimeter). As illustrated in Fig. 1, the losses in the various Nb_3Sn samples differ by as much as two orders of magnitude, an indication that particular processing methods or heat treatments determine the loss characteristics of the resultant Nb_3Sn. Curves a, b, and c show how the loss characteristics improve if Nb_3Sn samples are prepared by the composite process instead of the tin dipping process. Curve d shows results reported by Snowden and his co-workers (*3*) for a multilayered cylindrical Nb_3Sn specimen produced by electron-beam evaporation techniques. Curve e gives results for a sample of cylindrical niobium obtained during an investigation (*7*) to determine its suitability for a-c power transmission application. The composite process produces Nb_3Sn with lower losses than the electroplated niobium studied by the Linde group (*7*). The following conclusions may be drawn from the study reported here:

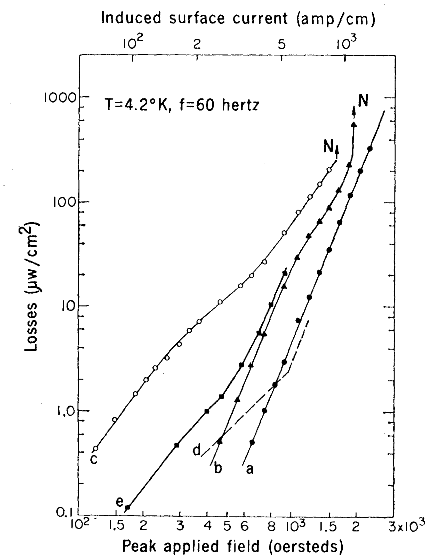

Fig. 1. Examples of a-c losses as functions of the peak applied magnetic fields and the induced root-mean-square current density in Nb_3Sn and niobium prepared by several processing techniques; *N*, normal. Curve a, Nb_3Sn prepared by the composite process with the sample heat-treated at 700°C for 66 hours (thickness, $\cong$ 2 μm); curve h, Nb_3Sn prepared by the tin dipping process heat-treated at 1000°C for 10 minutes (thickness, $\cong$ 1 to 2 μm); curve c, Nb_3Sn with 5 percent zirconium and 95 percent niobium prepared by the same process as that used in curve b; curve d, a multilayered Nb_3Sn prepared by an electron-beam evaporation technique (*3*); and curve e, niobium prepared for a transmission application (*7*). *N* indicates transition to the normal state.

1) Effect of the processing method: The Nb_3Sn samples made by the composite process exhibit substantially lower losses than those made by the tin dipping process. Studies of microstructures with an electron scanning microscope (*8*) and a transmission electron microscope (*9*) indicated that the grains of Nb_3Sn at its growth front are extremely fine (substantially less than 0.1 μm). Such fine grains are known to produce very high critical current densities in Nb_3Sn. Since it is believed that low a-c losses are associated with high critical current densities (*10, 11*) the low losses in Nb_3Sn prepared by the composite process are thought to be partly due to its fine grain sizes. In addition, microscopic study of the surfaces of the Nb_3Sn made by the tin dipping and the composite processes showed that the material produced by the tin dipping process had rougher surfaces than that produced by the composite process. This has led us to believe that low losses in the composite process Nb_3Sn may also be attributable to its smoother surface.

2) Effects of temperature and the time of Nb_3Sn formation: In both processes the higher losses are generally associated with the higher temperature of Nb_3Sn formation. However, the length of the heat treatment of the composite at a given temperature did not alter the losses appreciably, whereas, the longer the heat treatment for the tin dipping process the higher the losses.

3) Effects of impurities in the initial sample of niobium: The metallic purity of the initial niobium was 99.8+ percent, and the total gaseous impurities were less than 100 parts per million (by weight). In order to study the effects of metallic additions, small amounts of zirconium or hafnium [up to 6 percent (by weight)] were added to the niobium before the formation of Nb_3Sn. In general, the alloying metals added were deleterious and gave rise to higher a-c losses. One such example is shown in Fig. 1 (curve c); Nb_3Sn with 5 percent zirconium had much higher losses than Nb_3Sn without metallic additions.

4) Effects of niobium substrate on losses: In most of the tin dipped Nb_3Sn, losses due to niobium substrate at high fields ($\sim 1.5 \times 10^3$ oersteds) were observed, indicating the breakdown of the surface Nb_3Sn. However, similar losses were not observed in most of the composite Nb_3Sn. At any rate, the effects of niobium substrates on losses of Nb_3Sn were small for the magnetic field region of interest (0 to 1000 oersteds).

Most of the present theories on the a-c losses are based on the model of Bean (*10*) and London (*11*) or a modification of it (*12*). The theories state that the losses are hysteretic and depend on the peak magnetic field as H^n where $3 < n < 4$, depending on the model for the critical current density, $J_c(H)$. Our measurements of the frequency dependence of the losses (30 to 60 hertz) suggest that the observed losses are, in fact, hysteretic. However, the magnetic field dependence is much greater than predicted by the theories. In fact, n in most cases is larger than 4, and it is as large as 6 in some of the composite processed Nb_3Sn. The smaller values of n are observed only for those specimens with high losses, for example, Nb_3Sn with added impurities (curve c in Fig. 1). The effect of surface roughness also tends to decrease n. The present theories on a-c losses do not account for some of the observations reported here. A more detailed comparison of the theories and the present loss data will be given elsewhere (*13*).

After these encouraging results with rod specimens we decided to make several tape geometry Nb_3Sn conductors in lengths of 9.2 to 12.2 m by the composite process. Measurements performed on these tapes confirm that the losses in the composite processed tape are substantially lower than the best tapes produced by commercial suppliers. This result demonstrates that the losses in the improved conductors will not be significantly higher than other heat loads for a complete cable system, thus producing an optimized design. In addition, the composite process for making Nb_3Sn conductors does not require any new and relatively complex developments in technology such as vacuum evaporation techniques. In fact, it is possibly simpler than the two commercial methods commonly used to produce Nb_3Sn conductors, gas decomposition and tin dipping. Development of the low-loss Nb_3Sn described here makes its application to practical cables in the gigawatt range very attractive (*1, 5*). Such cables would have marked advantages with respect to higher operating temperature and fault current capability than cables employing a niobium conductor, and with the same or lower a-c loss.

M. SUENAGA
M. GARBER
Division of Metallurgy and Materials Science, Brookhaven National Laboratory, Upton, New York 11973

References and Notes

1. E. B. Forsyth, M. Garber, J. E. Jensen, G. H. Morgan, R. B. Britton, J. R. Powell, J. P. Blewett, D. H. Gurinsky, J. M. Hendrie, *Proceedings of the 1972 Applied Superconductivity Conference* (Institute of Electrical and Electronics Engineers, New York, 1972), p. 202 (this reference describes a conceptual coaxial transmission line made from Nb_3Sn ribbon conductor similar to that discussed in this report or made commercially).
2. M. Garber and W. B. Sampson, *Proc. 13th Int. Congr. Refrig.* (Paris) (1971), p. 393; M. J. Chant, M. R. Halse, H. O. Lorch, *Proc. Inst. Elec. Eng.* **117**, 1441 (1970).
3. C. H. Meyer, Jr., D. P. Snowden, S. A. Sterling, *Rev. Sci. Instrum.* **42**, 1584 (1971); D. P. Snowden, *Gulf Gen. At. Rep. No. 10281* (1962).
4. A. R. Kaufmann and J. J. Pickett, *Bull. Am. Phys. Soc.* **15**, 838 (1970); M. Suenaga and W. B. Sampson, *Appl. Phys. Lett.* **18**, 584 (1971).
5. E. B. Forsyth, Ed., *Brookhaven Natl. Lab. Rep. No. 50325* (1972).
6. R. M. Easson and P. Hlawiczka, *Br. J. Appl. Phys.* **18**, 1237 (1967).
7. H. M. Long, W. T. Beall, Jr., L. K. Eigenrod, R. W. Meyerhoff, J. Notaro, "Superconducting Cable System, EEI Project RP 78-7" (final report, Edison Electric Institute, New York, October 1969); R. W. Meyerhoff and W. T. Beall, Jr., *J. Appl. Phys.* **42**, 147 (1971).
8. H. H. Farrell, G. H. Gilmar, M. Suenaga, unpublished data.
9. R. Scanlan, personal communication; B. Park and M. Suenaga, unpublished data.
10. C. P. Bean, *Rev. Mod. Phys.* **36**, 31 (1964).
11. H. London, *Phys. Lett.* **6**, 162 (1963).
12. For a summary, see P. H. Melville, *Phil. Mag.* **27**, 647 (1973).
13. M. Suenaga, M. Garber, J. Bussiére, in preparation.
14. We thank D. H. Gurinsky, E. B. Forsyth, and W. B. Sampson for helpful discussions and guidance. We also thank S. Shen for measurements and C. Klamut, A. Cendrowski, D. Horne, F. Iseli, R. Mitchell, and S. Pollack for expert technical assistance. This work was carried out under the auspices of the National Science Foundation and the Divisions of Physical Research and Applied Technology of the U.S. Atomic Energy Commission.

15 October 1973; revised 17 December 1973

Melting Relations of the Allende Meteorite

Abstract. *The proportions of major oxides in the Allende carbonaceous chondrite after partial reduction are remarkably similar to those in possible mantle material of the earth. When heated, the Allende meteorite generates a sulfide melt (47 percent iron, 25 percent nickel, and 24 percent sulfur by weight), a ferrobasaltic melt, and olivine with or without pyroxene, over a wide pressure range (5 to 25 kilobars). The silicate melt contains more sodium and less titanium than lunar ferrobasalts. An aggregate of the Allende chondrite rich in calcium and aluminum produces silica-undersaturated, calcium-rich melt and spinel over a wide pressure and temperature range. From these studies, it is suggested that the earth's core contains significant amounts of both nickel and sulfur and that a 3 : 2 mixture of Allende bulk sample and calcium- and aluminum-rich aggregates is closer in major element abundances than either of these components to the average composition of the moon.*

The carbonaceous chondrites are believed to be the most undifferentiated condensed material in the solar system (*1*). If planets formed by accretion of material having solar proportions of the condensed elements, heating and melting experiments with a carbonaceous chondrite should reproduce the events that would have taken place in the early evolution of these planets.

Table 1. Chemical composition of the Allende meteorite after partial loss of oxygen and extraction of the metallic phase compared with that of possible mantle material. The Allende material was analyzed by Clarke *et al.* (*3*) after subtracting 4.73 percent oxygen, 19.2 percent iron, 1.45 percent nickel, and 2.21 percent sulfur. Peridotite analysis is by Kuno and Aoki (*5*).

Oxide	Percentage in	
	Allende meteorite	Salt Lake peridotite
SiO_2	46.50	48.3
TiO_2	0.22	0.22
Al_2O_3	4.56	4.91
Cr_2O_3	0.70	0.25
FeO	9.91	9.95
MnO	0.24	0.14
MgO	33.31	32.5
CaO	3.59	2.99
Na_2O	0.60	0.66
K_2O	0.04	0.07
P_2O_5	0.32	

Many considerations have been advanced to support the premise that the earth has a composition similar to that of some chondritic meteorites (*2*). Further evidence that the proportions of major elements of at least the silicate fraction of the earth are similar to those of one group of carbonaceous chondrites is presented in Table 1. The composition of the silicate portion of the Allende type 3 carbonaceous chondrite (*3*) after reduction of 19.7 percent of the iron oxide to metallic iron is given in Table 1. For comparison, the composition of a peridotite inclusion from a tuff of the Salt Lake Crater, Hawaii, is also presented. On being heated, this rock produces tholeiite and alkali basaltic melts at pressures from 10 to 20 kbar (*4*) and is believed to be representative of the oceanic upper mantle (*5*). The composition of the partially reduced silicate phase of the Allende